International Journal of Biological Macromolecules 248 (2023) 125886

Contents lists available at ScienceDirect

International Journal of Biological Macromolecules

journal homepage: www.elsevier.com/locate/ijbiomac

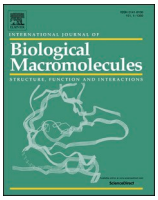

Influence of dispersion of fibrillated cellulose on the reinforcement of coated papers

Jose Luis Sanchez-Salvador [a,b], Maria Graça Rasteiro [b], Ana Balea [a], Mohit Sharma [b], Jorge F.S. Pedrosa [b], Carlos Negro [a], M. Concepcion Monte [a], Angeles Blanco [a,*], Paulo J.T. Ferreira [b]

[a] Department of Chemical Engineering and Materials, Universidad Complutense de Madrid, Avda. Complutense s/n, 28040 Madrid, Spain
[b] Department of Chemical Engineering, CIEPQPF, University of Coimbra, Rua Sílvio Lima, 3030-790 Coimbra, Portugal

ARTICLE INFO

Keywords:
Cellulose nanofibers
Dispersion degree
Rheology of nanocellulose coating formulations

ABSTRACT

The use of cellulose micro/nanofibrils (CMNFs) as reinforcement paper additive at industrial scale is delayed due to inconsistent results, suggesting a lack of proper consideration of some key parameters. The high influence of fibrillated nanocellulose dispersion has been recently identified as a key parameter for paper bulk reinforcement but it has not been studied for surface coating applications yet. This paper studies the effect of CMNF dispersion degree prior to their addition and during mixing with starch on the reinforcement of paper by coating. Results show that this effect depends on the type of CMNFs since it is related to the surface interactions. For a given formulation, a correlation is observed between the CMNF dispersion and the CMNF/starch mixing agitation with the rheology of the coating formulation which highly affects the paper properties. The optimal dispersion degree is different for each nanocellulose, but the best mechanical properties were always achieved at the lowest viscosity of the coating formulation. In general, the initial state of the nanocellulose 3D network, influences the mixing and smooth application of the coating and affects the reinforcement effect. Therefore, the CMNF industrial implementation in coating formulations will be facilitated by the on-line control of formulations prior to their surface application.

1. Introduction

The development of new materials and composites requires an adequate characterization in terms of properties, reactivity, morphology and composition [1]. This applies to the disintegration of cellulose fibers into smaller substructures, which results in several cellulose micro and nanofibrillated materials, including cellulose micro and nanofibrils (CMNFs) [2]. CMNFs are suitable for a wide range of applications due to their excellent properties, including high surface area, high mechanical strength, high aspect ratio, excellent barrier properties, renewable nature, and the ability to undergo functionalization [3–5]. CMNFs have been widely studied during the last two decades as a promising material in multiple fields, as evidenced by the large amount of research at lab scale [6,7]. Among these fields, in sectors such as paper and cardboard, cement or in polymeric composites, the CMNF use is mainly focused on the reinforcement of these materials to improve their structural and mechanical properties. Although they have also additional potential applications such as in environmental remediation, due to the adsorption capacity of pollutants (e.g. metals, dyes, emerging contaminants); in food and cosmetic industries, as stabilizer due to their amphiphilicity or as rheology modifiers due to their shear-thinning behaviour; as drug carriers in pharmaceutical industry or in biomedical applications as wound healing or as scaffold in tissue engineering [3,8].

However, the only large-scale application nowadays is in paper and board manufacturing. CMNFs can be applied both in bulk and in paper surface treatments, either alone or as a component of a blending mixture [9]. However, despite successful results of CMNF application at lab scale, which include significant increments of the mechanical properties of paper and cardboard sheets, their industrial implementation is still facing challenges that need to be addressed to unlock their full potential [10]. One of the major challenges is the inconsistency and variability of the data obtained in different studies, suggesting that some key parameters, namely the dispersion degree of CMNFs prior to its application or their mixing with the polymeric matrices, are not taken into

* Corresponding author.
E-mail address: ablanco@ucm.es (A. Blanco).

https://doi.org/10.1016/j.ijbiomac.2023.125886
Received 25 May 2023; Received in revised form 21 June 2023; Accepted 9 July 2023
Available online 20 July 2023

Table 1
Characterization of the CMNFs produced.

	M-CMFs	M-CMNFs	T-CNFs
Carboxyl groups (mmol COOH/g)	0.15 ± 0.01	0.28 ± 0.04	1.45 ± 0.06
Transmittance 600 nm (%)	9.5 ± 0.9	11.0 ± 0.2	87.8 ± 0.1
Cationic Demand (μeq/g)	76 ± 9	144 ± 18	1705 ± 12
Polymerization degree (N° monomers)	1186 ± 13	1049 ± 49	191 ± 9
Ashes (%)	<1 %	<1 %	9.9 ± 0.1

consideration [11–13]. Some studies have indicated the importance of avoiding CMNF aggregates, obtaining a good dispersion and uniformity of the three-dimensional CMNF networks, which produces better results in the mechanical properties of the final products [13–15]. Dispersion can be improved mechanically [11,14] or by using chemical dispersants [13,14].

There are not direct methods to determine the dispersion degree of CMNF gels in water suspensions prior to their application into polymer matrices. Some authors have used indirect measurement such as sedimentation measurements, air permeability, optical transmittance or visualization of aggregates in microscopy images [13,14,16,17], but they are scarce and qualitative. Furthermore, they do not consider the potential break down of the fibers beyond the network separation under high shear forces.

In a previous work, the hypothesis that the agitation used to prepare CMNF suspensions has an impact on the entanglement network and on the separation of fibrils was confirmed using the gel point methodology [11]. This methodology was applied to evaluate the degree of dispersion of CMNFs for bulk reinforcement of recycled cardboard. The optimal conditions to improve the mechanical properties of cardboard were obtained when the CMNF dispersion was carried out independently of the pulping process. The best dispersion was obtained with an intermediate agitation of the 3D CMNF network corresponding to the minimum value of the gel point, that coincide with the maximum aspect ratio (AR), since the maximum improvements of the cardboard mechanical properties were obtained. These conditions ensured the absence of fiber clusters produced at lower agitations and prevented the mechanical breakage of the fibril network at higher agitation speeds. The optimal CMNF dispersion allow us to obtain an additional 18 % increase of the tensile index of the reinforced recycled cardboard.

The favourable results of the dispersion degree study of CMNFs before their bulk application on cardboards suggest that this factor may also significantly influence other applications, such as the surface application of CMNFs. The use of CMNFs in the surface reinforcement of base papers has been applied both on their own in some instances [18], as well as in coating formulations, blended with other coating materials such as starch or carboxymethyl cellulose. These blends favour obtaining easy to apply coatings, avoiding the quick absorption of the CMNF suspension in the based paper and also obtaining better mechanical properties than when the CMNFs are applied on their own [19,20]. In this study, the dispersion degree of coatings formulated with starch and different types of CMNFs has been investigated considering, first, the dispersion degree of the CMNFs before its use, second, the mixing of the CMNFs with the starch and, finally, its effect on paper properties.

2. Materials and methods

Eucalyptus globulus bleached kraft pulp (Torraspapel, S.A., Zaragoza, Spain), with 74.5 wt% of cellulose and 16.9 wt% of hemicellulose [21],

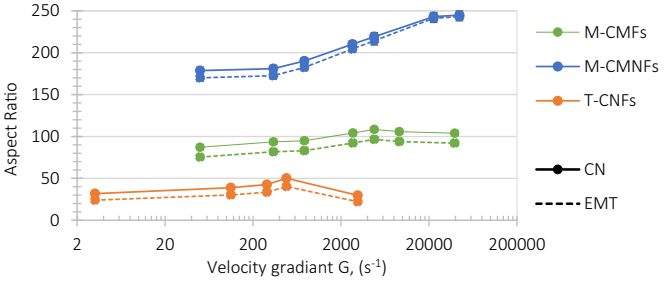

Fig. 2. Aspect ratio of the CMNF suspensions at different stirring speed using the crowding number (CN) and effective medium theories (EMT).

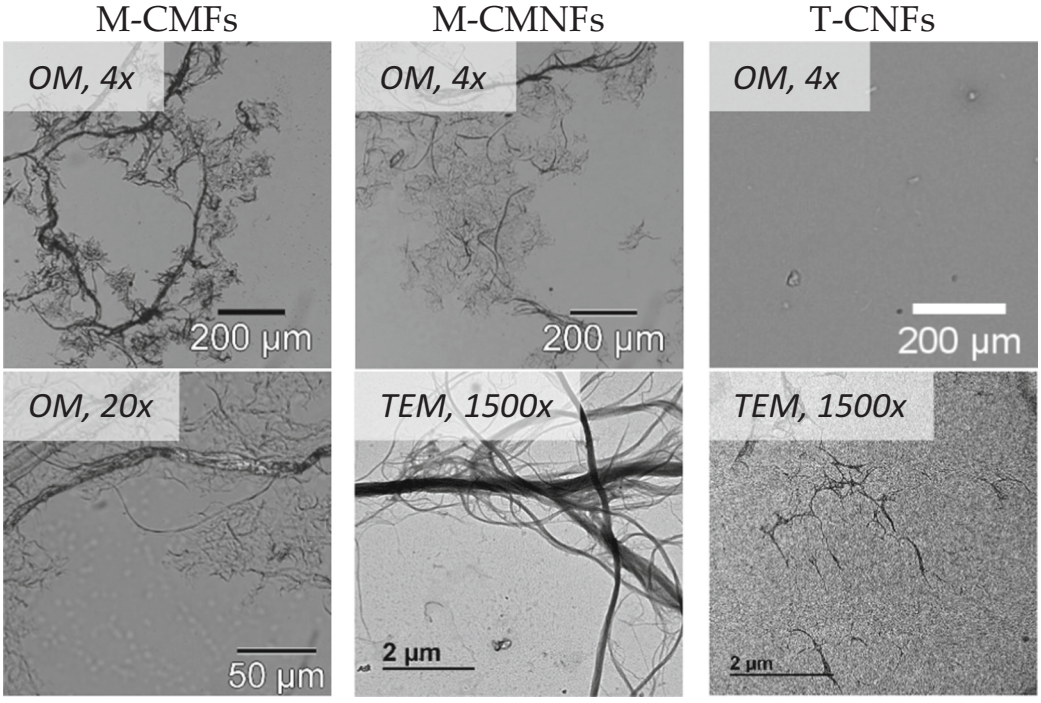

Fig. 1. Optical microscopy (OM) and transmission electron microscopy (TEM) of the different fibrillated cellulose used.

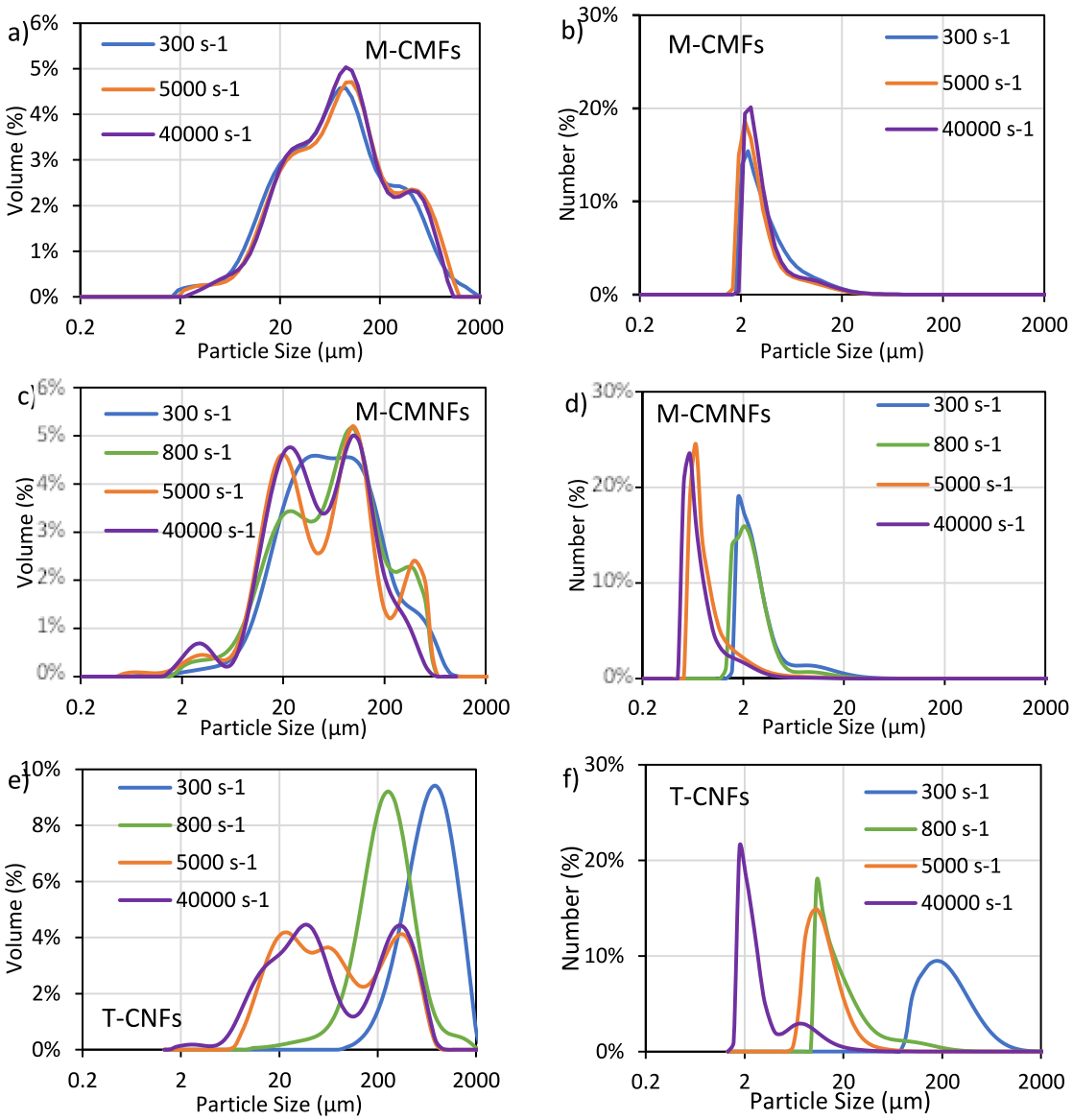

Fig. 3. Particle size distribution in volume (a, c and e) and number (b, d and f) of CMNF suspensions at different stirring speeds using LDS.

was used as the raw material to produce different CMNFs. The base paper used for coating was filter paper 1305 with a grammage of 73 g/m^2 (Filtros Anoia, Barcelona, Spain). Corn native starch of industrial origin, with 27.3 wt% of amylose, was used. Other chemicals used in the preparation of the cellulose nanofibrils (CNFs) chemically pretreated (T-CNFs) were 2,2,6,6-Tetramethylpiperidine-1-oxyl (TEMPO) (Sigma Aldrich, St. Louis, MO, USA) and NaBr as catalysts in the TEMPO-mediated oxidation (TMO). NaClO solution, previously titrated to determine the hypochlorite concentration, and NaOH were purchased from Panreac AppliChem (Barcelona, Spain). For the CMNFs characterization, cupriethylenediamine solution (CED), also supplied by Panreac AppliChem, was used for the polymerization degree characterization, and 0.1 wt% poly-L-lysine solution (Electron Microscopy Sciences, Hatfeld, PA, USA) was used for transmission electron microscopy (TEM) analysis.

In this study, three different types of CMNF suspensions were evaluated: chemically pretreated CNFs (T-CNFs), mechanically pretreated cellulose microfibrils (M-CMFs) and mechanically pretreated cellulose micro and nanofibrils (M-CMNFs). In all cases, cellulose pulp was firstly soaked in water for 24 h to promote fiber swelling. Then, the pulp was disintegrated using a pulp disintegrator (PTI, Vorchdorf, Austria) according to ISO 5263-1 standard [22]. For the production of M-CMFs, the pulps were refined at 20,000 revolutions in a PFI mill (Hamjem Maskin AS, Hamar, Norway), adjusting the pulp consistency to 10 wt% according to the ISO 5264-2 standard [23]. To produce M-CMNFs, the M-CMF suspension, at 1 % of consistency, was homogenized in a high-pressure laboratory homogenizer (HPH) PANDA PLUS 2000 manufactured by GEA Niro Soavy (Parma, Italy) using three passes at 300, 600 and 900 bar. Finally for T-CNFs, TMO was carried out according to the conditions described by Saito et al. (2007) using a glass reactor, with 1 wt% cellulose, 0.1 mmol TEMPO/g pulp and 1 mmol NaBr/g pulp [16]. 3 mmol NaClO per gram of pulp were added to start the reaction. The pH of the reaction was adjusted around 10 using NaOH until a constant pH was reached, indicating the complete consumption of NaClO [24]. Then, the oxidized pulp was washed until neutral pH with distilled water and filtered using a nylon mesh. Similar to M-CMNFs, three passes of HPH were applied at 300, 600 and 900 bar.

Afterwards, the CMNFs were characterized using the following parameters. Optical transmittance: CMNF suspensions were prepared at 0.1 wt% and the optical transmittance was measured using a Cary 50 Conc UV–Visible spectrophotometer (Varian Australia PTI LTD, Victoria, Australia) at 600 nm. Polymerization degree: determined by

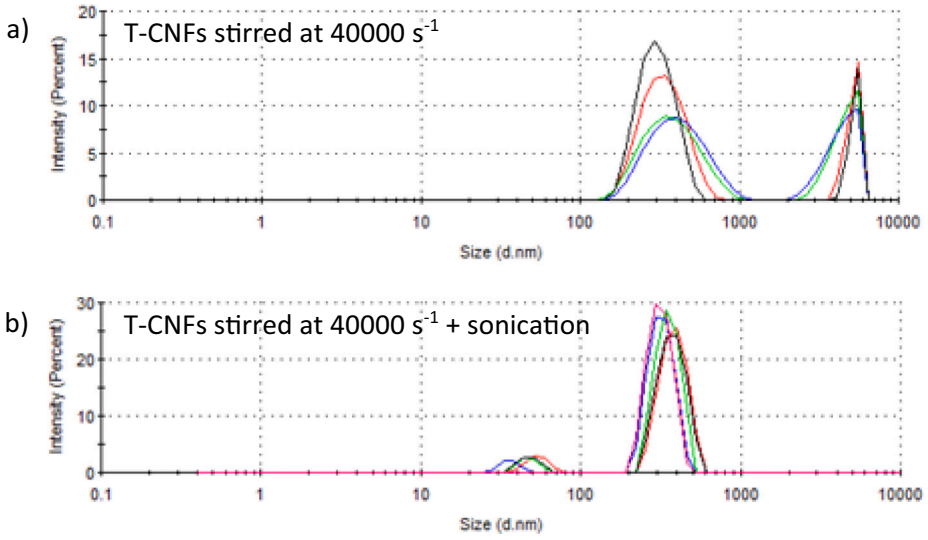

Fig. 4. Particle size of T-CNFs using DLS. The different colors correspond to distinct replicates of the same analysis.

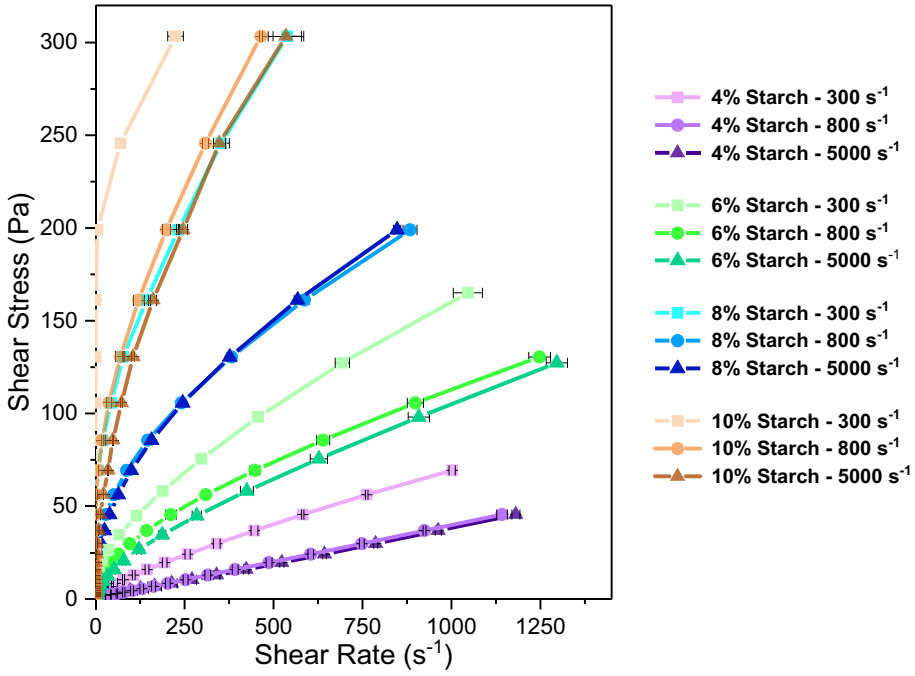

Fig. 5. Shear stress vs. shear rate of different starch suspensions at different concentrations in terms of weight and stirring agitations.

Table 2
Mechanical and structural properties of papers coated with starch at different concentrations in weight and agitations.

	Thickness (mm)	Gurley air resistance (s)	Tensile Index (Machine Direction) (kN·m/kg)	Tensile Index (Cross Direction) (kN·m/kg)	Tear Index (mN·m^2/g)
Base paper	0.145 ± 0.006	1.5 ± 0.1	35.3 ± 1.8	26.6 ± 1.6	10.68 ± 0.70
6 % 300 s^{-1}	**0.150 ± 0.006**	**421 ± 70**	**49.1 ± 2.2**	**39.4 ± 0.8**	**10.59 ± 0.12**
6 % 5000 s^{-1}	0.148 ± 0.004	83 ± 4	45.1 ± 0.9	38.0 ± 2.1	10.61 ± 0.36
8 % 300 s^{-1}	0.161 ± 0.008	1948 ± 18	43.1 ± 1.7	36.2 ± 2.6	10.81 ± 0.59
8 % 5000 s^{-1}	0.158 ± 0.004	746 ± 140	41.8 ± 3.3	32.8 ± 1.6	10.84 ± 0.54

Bold row means the best mechanical results.

intrinsic viscosity measurements according to ISO 5351, by dissolving cellulose in a CED solution [25]. Carboxyl groups content: determined by conductometric titration, in which 0.15 g of dry CMNFs were mixed with 5 mL of 0.01 M NaCl, and deionized water was added until the final volume reached 55–60 mL. The pH was adjusted to 2.7–2.9 using 0.1 M HCl to protonate carboxyl groups, then titrated using 0.05 M NaOH (in 0.2 mL increments) to the sample, and the conductivity after each addition was recorded [26]. Cationic demand (CD): determined by using

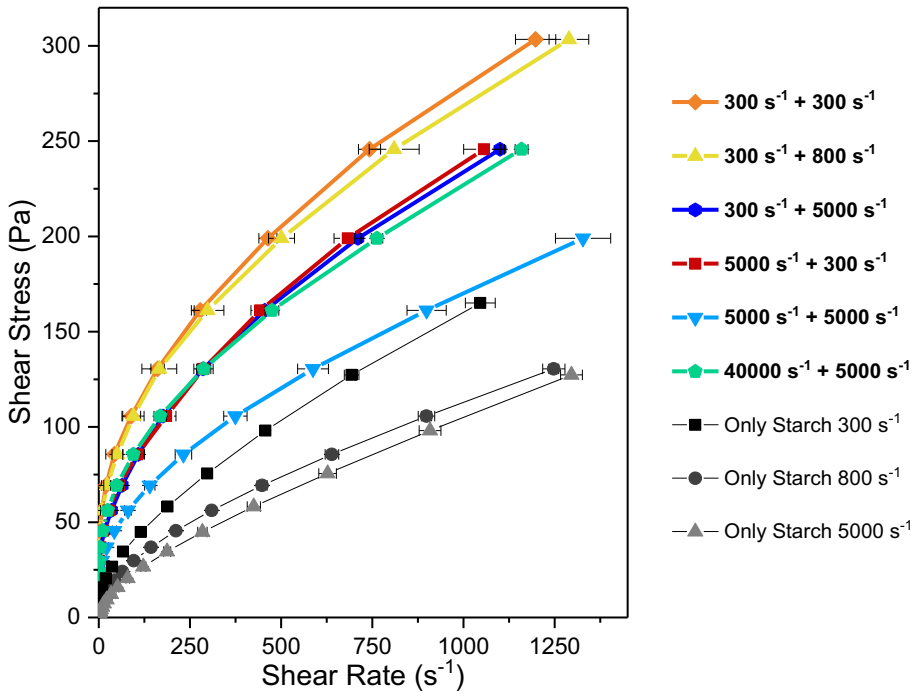

Fig. 6. Rheology of coatings prepared at 6 wt% of total solids corresponding to 20 wt% of M-CMFs and 80 wt% of starch with different agitation speeds: agitation of M-CMF suspension + M-CMF/starch mixture agitation.

back titration with a charge analyzing system (AFG Analytic GmbH, Leipzig, Germany) [27]. Ash content: determined by calcination according to TAPPI T211 standard [28]. Morphological characterization: a polarized light optical microscope Olympus BH-2 KPA (Olympus Optical Co., Ltd) equipped with a high-resolution CCD colour camera (Olympus ColorView III) was used for the M-CMFs and M-CMNFs characterization. For T-CNFs, TEM was carried out at the Centro Nacional de Microscopía Óptica (Madrid, Spain) with a JEM 1400 microscope using copper grids covered with a formvar/carbon continuous layer and Poly-L-Lysine [29].

The dispersion of CMNFs at different stirring speeds was evaluated using a simplified gel point methodology, which requires only one initial concentration (C_o) to obtain the AR of the fibrils [30,31]. For the sedimentation experiments, suspensions with different hydrogels were prepared by mixing deionized water with 200 μL of 0.1 wt% crystal violet to dye the fibers. The samples were agitated at several velocity gradients using an overhead stirrer Heidolph RZR 2051 (Heidolph Instruments, Schwabach, Germany) or a Dispermat disperser® CV3-PLUS-E (VMA-Getzmann, Reichshof, Germany) for intense agitations. Then, 250 mL of each suspension were poured into graduated cylinders and allowed to settle until the sediment reached a stable value over time, corresponding to the complete deposition of the suspension. As described by Sanchez-Salvador et al. (2021), relative heights (sediment/total height, H_s/H_o) were used to estimate the gel point ($Ø_g$) according to Eq. (1) [31].

$$\text{Gel point}, Ø_g\left(\frac{kg}{m^3}\right) = \lim_{H_s/H_o \to 0}\left(\frac{dC_o}{d\left(H_s/H_o\right)}\right) \approx \frac{C_o(i) - C_o(0)}{\left(H_s/H_o(i)\right) - \left(H_s/H_o(0)\right)} = \frac{C_o(i)}{\left(Hs/Ho(i)\right)} \quad (1)$$

From gel point value is possible to calculate the average AR of the CMNFs according to the Crowding Number (CN) and to the Effective Medium Theory (EMT) using Eq. 2 and Eq. 3, respectively [11,32,33].

$$\text{Aspect ratio, AR (CN)} = 5.98 \bullet \sqrt{\frac{1000}{\text{Gel point}, Ø_g\left(\frac{kg}{m^3}\right)}} \quad (2)$$

$$\text{Aspect ratio, AR (EMT)} = 3.61 \bullet \left(\frac{1000}{\text{Gel point}, Ø_g\left(\frac{kg}{m^3}\right)}\right)^{0.567} \quad (3)$$

In addition, laser diffraction spectroscopy (LDS) was used to analyze the particle' size of samples, for particles larger than 1 μm, using a Mastersizer 2000 (Malvern Instruments, Malvern, United Kingdom) equipped with a Hydro 2000MU module [34]. The CMNF suspensions, previously stirred at different speeds, were analyzed using a pump speed of 2000 rpm. On average, five measurements were carried out. Since LDS only detects particles in the micrometer range, which is the case of M-CMFs or the fraction of the M-CMNF suspensions that have not been completely fibrillated or that exist in the form of clusters or aggregates [35,36], dynamic light scattering (DLS) measurements were performed to characterize the nanosize T-CNFs, using a Zetasizer Nano ZS equipment, also from Malvern Instruments. The samples were diluted to 0.1 wt% and carefully transferred to a glass cuvette avoiding the presence of bubbles, and then the particle size was measured.

For the preparation of the coating formulations, the CMNFs proportions were selected according to a recent study conducted by Sharma et al. (2022), who found that CMNF concentrations up to 32 wt% resulted in uniform coatings, with the optimal value established at 16 wt % CMNFs [20]. Based on these findings, in the present study the coating suspensions were prepared with 20 wt% of M-CMFs, M-CMNFs or T-CNFs and 80 wt% of native starch.

In addition, to prepare the coatings, a solid content of 6 wt% was selected, except for T-CNFs, which had a higher viscosity, requiring a reduction of the total solids content to 4 wt%. First, CMNF gels were stirred with water with a high-speed overhead stirrer Heidolph RZR 2051 at different values for 10 min while simultaneously heating the mixture to 90 °C using a hot water bath. For the highest agitation speeds, the Dispermat disperser® CV3-PLUS-E was used (VMA-Getzmann

Table 3
Mechanical properties of the base paper coated with 20 wt% of M-CMFs and 80 wt% of starch. Equal superscripts for the same property indicate samples with no significant differences according to the Multiple Range Test.

	Tensile Index (Machine Direction) (kN·m/kg)	Tensile Index (Cross Direction) (kN·m/kg)	Burst Index (kPa·m^2/g)	Tear Index (mN·m^2/g)	Gurley air resistance (s)
Base paper	35.3 ± 1.8^{a}	26.6 ± 1.6^{a}	1.56 ± 0.13^{a}	10.28 ± 0.39^{a}	1.5 ± 0.1^{a}
Only Starch 300 s^{-1}	49.1 ± 2.2^{c}	39.4 ± 0.8^{b,c}	3.09 ± 0.14^{c}	10.59 ± 0.12^{a,b}	421 ± 70^{d}
Only Starch 5000 s^{-1}	45.1 ± 0.9^{b}	38.0 ± 2.1^{b}	2.69 ± 0.11^{b}	10.44 ± 0.18^{a,b}	83 ± 4^{b}
300 s^{-1} + 300 s^{-1}	51.3 ± 2.3^{c,d}	39.3 ± 2.2^{b}	3.14 ± 0.20^{c}	10.57 ± 0.39^{a,b}	134 ± 34^{b,c}
300 s^{-1} + 800 s^{-1}	51.3 ± 1.6^{c,d}	38.3 ± 1.0^{b}	3.25 ± 0.24^{c}	10.69 ± 0.62^{b}	148 ± 46^{b,c}
300 s^{-1} + 5000 s^{-1}	56.1 ± 1.2^{f}	41.3 ± 2.2^{c}	3.54 ± 0.22^{d}	10.58 ± 0.35^{a,b}	208 ± 106^{c}
5000 s^{-1} + 300 s^{-1}	53.2 ± 2.4^{d,e}	39.4 ± 1.6^{b}	3.11 ± 0.12^{c}	10.56 ± 0.25^{a,b}	127 ± 56^{b,c}
5000 s^{-1} + 5000 s^{-1}	**55.1 ± 1.7^{e,f}**	**46.9 ± 1.7^{d}**	**3.75 ± 0.13^{e}**	**11.04 ± 0.44^{c}**	**444 ± 94^{d}**
40,000 s^{-1} + 5000 s^{-1}	55.6 ± 2.9^{f}	39.9 ± 1.2^{b,c}	3.50 ± 0.23^{d}	10.59 ± 0.82^{a,b}	188 ± 88^{c}

Bold row means the best mechanical properties.

GmbH, Reichshof, Germany). Next, a starch solution with a concentration of 10 wt% was added to the CMNFs using different agitation speeds for the mixture, at a temperature of 90–95 °C for 10 min. During the preparation, water evaporation was controlled to maintain the desired solids percentage. Then, the temperature was reduced to 50 °C before the surface coating.

The rheology of the coating suspensions was analyzed using a controlled stress rheometer (Haake RS1, Karlsruhe, Germany) with a plate geometry (PP20-Ti) sensor. For each condition an average value was obtained by preparing three times each mixture and performing at least three times each rheology test. Then, the coating formulations were applied using a Mathis laboratory coating device (Oberhasli, Switzerland), with a pre-drying infrared system coupled to an applicator bar (SVA-IR-B). Finally, the coated sheets were air dried at room temperature.

Some structural and mechanical properties of the coated paper were measured. The air resistance was evaluated using the Gurley method described in the ISO 5636-3 standard [37]. The mechanical properties were assessed by measuring the tensile index (kN·m/kg), the tear index (mN·m^2/g) and the burst index (kPa·m^2/g), according to the corresponding ISO standards [38–40]. To evaluate the significance of the results, the Multiple Range Test of Least Significant Difference (LSD) was carried out using the Statgraphics Centurion 19 software with the analysis of variance (ANOVA) tool. Optical microscopy (OM) of the coating films produced on a plastic surface, without the base paper, was also evaluated by using the polarized light optical microscope Olympus.

3. Results and discussion

To study the effect of the dispersion of the fibrillated suspensions on coatings, CMNFs and starch were first tested independently. Table 1 shows the properties of the three CMNFs that were studied. Among them, T-CNFs show the most distinct characteristics due to the chemical pretreatment. This pretreatment increased the number of carboxyl groups to 1.45 mmol/g pulp on the surface of the fiber, enhancing the electrostatic repulsion among fibrils. This led to an almost total fibrillation when subjected to the HPH process, yielding highly individualized nanofibers with a lower PD compared to the mechanical pretreatment samples [41]. On the other hand, both M-CNFs and M-CMNFs were obtained without any chemical pretreatment for fibrillation and exhibit typically lower amounts of carboxyl groups compared to T-CNFs. Fig. 1 shows the optical microscopy (OM) images and transmission electron microscopy (TEM) images of the fibrillated celluloses produced. OM images show higher fibrillation for M-CMNFs than for M-CMFs. In the M-CMNF sample, a fraction of fibrils existed in the microscale, while another fraction falls between the micro and nanoscale as a result of the HPH fibrillation treatment as shown in the TEM image, which slightly reduced the average number of monomers in each chain from 1186 to 1049. In the case of M-CMFs, since all fibers are in the microscale, TEM images do not provide any information, so OM images are displayed at 4× and 20×. On the contrary, in the case of T-CNFs, OM only shows a few aggregates since most of the fibers are in the nanoscale. As for the ash content, it is observed an increase in the amount of ashes after the TMO process due to the presence of sodium

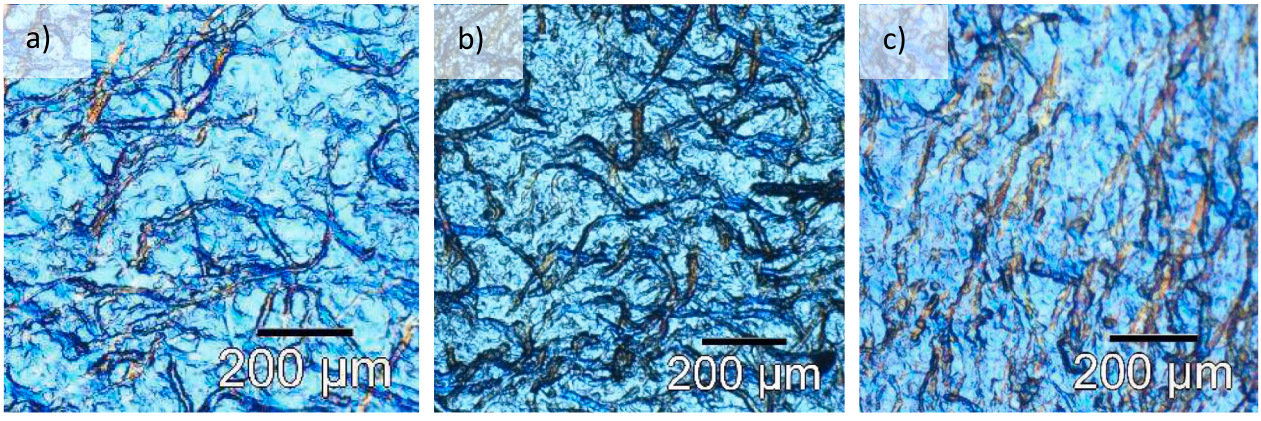

Fig. 7. Optical microscopy of coatings prepared at 6 wt% of total solids with 20 wt% of M-CMFs and 80 wt% of starch with different agitations of the M-CMF and the mixture: a) 300 s^{-1} + 300 s^{-1}; b) 5000 s^{-1} + 5000 s^{-1}; c) 40,000 s^{-1} + 5000 s^{-1}.

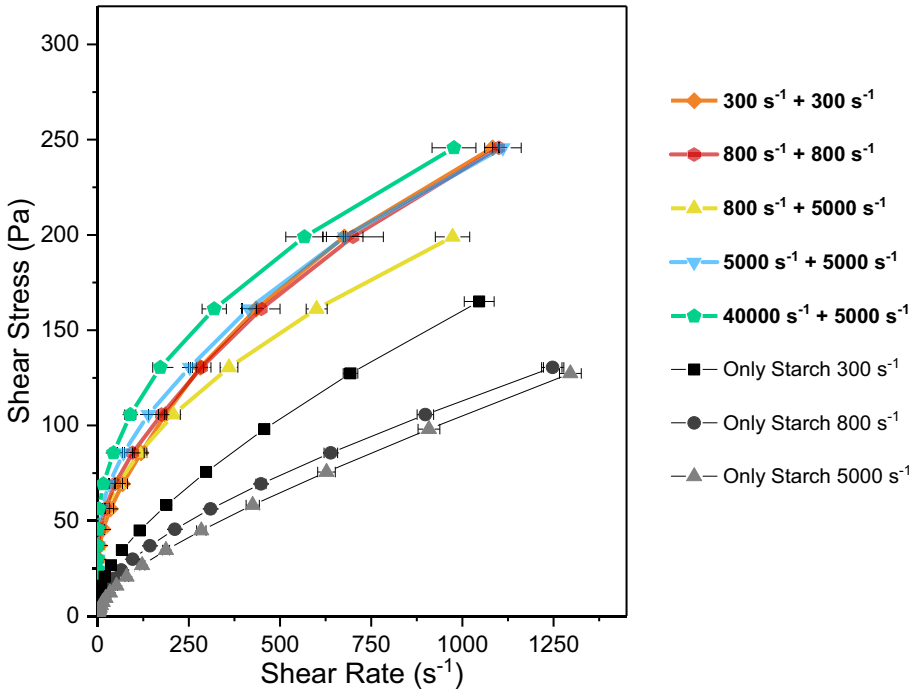

Fig. 8. Rheology of coatings prepared at 6 wt% of total solids with 20 wt% of M-CMNFs and 80 wt% of starch with different agitation speeds: agitation of M-CMNF suspension + M-CMNF/starch mixture agitation.

Table 4
Mechanical properties of base paper coated with a mixture of 20 wt% of M-CMNFs and 80 wt% of starch.

	Tensile index (Machine Direction) (kN·m/kg)	Tensile index (Cross Direction) (kN·m/kg)	Burst index (kPa·m^2/g)	Tear index (mN·m^2/g)	Gurley air resistance (s)
Base paper	35.3 ± 1.8^a	26.6 ± 1.6^a	1.56 ± 0.13^a	10.28 ± 0.39^a	1.5 ± 0.1^a
Only Starch 300 s^{-1}	49.1 ± 2.2^c	39.4 ± 0.8^b	3.09 ± 0.14^c	10.59 ± 0.12^{a,b}	421 ± 70^c
Only Starch 5000 s^{-1}	45.1 ± 0.9^b	38.0 ± 2.1^b	2.69 ± 0.11^b	10.44 ± 0.18^{a,b}	83 ± 4^b
300 s^{-1} + 300 s^{-1}	52.6 ± 2.0^d	40.2 ± 2.2^b	3.45 ± 0.13^d	10.77 ± 0.53^b	91 ± 39^b
800 s^{-1} + 800 s^{-1}	55.3 ± 2.8^d	45.4 ± 1.2^c	3.81 ± 0.11^e	10.93 ± 0.45^b	97 ± 1^b
800 s^{-1} + 5000 s^{-1}	**57.0 ± 0.8^e**	**45.4 ± 1.9^c**	**3.96 ± 0.17^f**	**10.91 ± 0.43^b**	**655 ± 150^d**
5000 s^{-1} + 5000 s^{-1}	54.4 ± 3.1^d	42.9 ± 1.1^d	3.51 ± 0.15^d	10.74 ± 0.48^b	635 ± 193^d
40,000 s^{-1} + 5000 s^{-1}	54.5 ± 1.6^d	43.1 ± 1.3^d	3.53 ± 0.26^d	10.76 ± 0.43^b	671 ± 93^d

Bold row means the best mechanical properties.

chloride that is added in the commercial NaClO to improve its stability during storage and also another part is produced in parallel during the TEMPO-mediated oxidation reaction. These salts remain attached to the fibers and are not completely removed during the washing step [42,43].

On the other hand, the AR of the fibrils was calculated at different stirring speeds (Fig. 2) using the simplification of the gel point method [31]. As expected, M-CMNFs exhibit a higher number of branches along the cellulose backbone due to the effect of refining before the homogenization, resulting in the highest AR compared with other pretreatment methods such as enzymatic hydrolysis or TEMPO-mediated oxidation [43]. On the other hand, T-CNFs have the lowest AR because the TMO chemical pretreatment oxidizes the cellulose, which favours the repulsion among the fibrils and, at the same time, the breaking of the glycosidic bonds, reducing the number of monomers in the cellulose chains [44].

Regarding the agitation, the AR show a similar trend in the three samples, with a maximum value corresponding to the minimum gel point, since both magnitudes are inversely proportional [11]. At low agitation, the hydrogels are barely mixed, and the fibrils begin to separate in different ways, depending on the treatment. As the shear forces increase, the relative height in the sedimentation experiments increases compared to the sample without agitation, indicating that the 3D CMNF structures become more open and spongier with the dispersion of clusters. However, there is a limit to this effect: if agitation is too high, the 3D network can collapse, as shown by the compaction of the sediment at the base of the graduated cylinders, due to the breaking of hydrogen bonds between fibrils and subsequent fibrils separation. Furthermore, high agitation may also shorten the fibrils [12]. Nevertheless, this decrease in the AR with the increasing velocity gradient is mainly observed in highly fibrillated nanocellulose, such as in the case of T-CNFs, where the maximum AR value is obtained at around 500 s^{-1}. The viscoelastic hydrogel formed after homogenization leads to a relative low agitation able to break the gel networks, resulting in a reduction in the viscosity [45].

However, when fibrillation was produced mechanically, a higher agitation was required to obtain the maximum AR. The shaking forces not only dispersed the fibrils but also produced the fibrillation of the

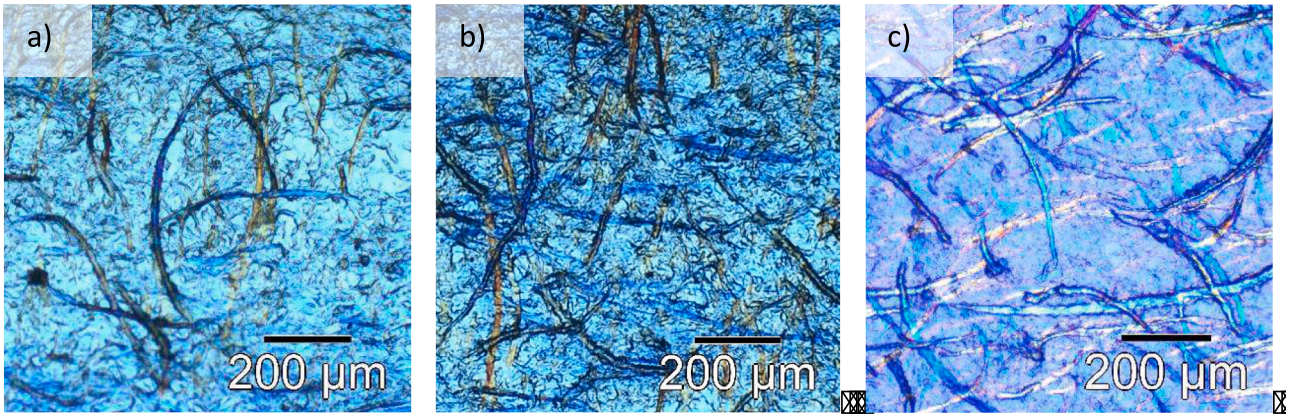

Fig. 9. Optical microscopy of coatings prepared at 6 wt% of total solids with 20 wt% of M-CMFs and 80 wt% of starch with different M-CMF and mixture agitations: a) 300 s^{-1} + 300 s^{-1}; b) 800 s^{-1} + 5000 s^{-1}; c) 40,000 s^{-1} + 5000 s^{-1}.

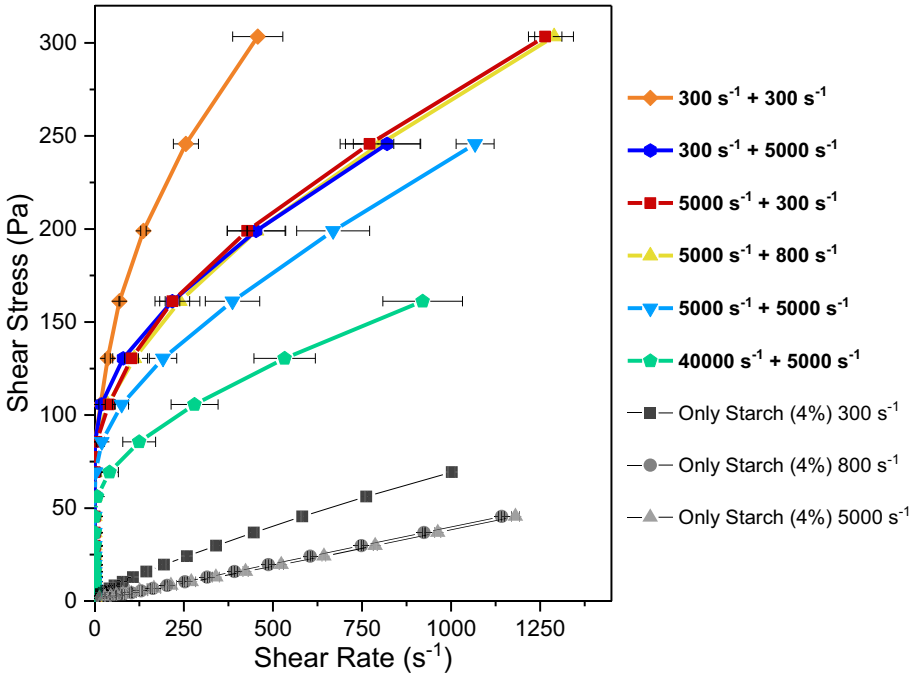

Fig. 10. Rheology of coatings prepared at 4 wt% of total solids with 20 % of T-CNFs and 80 % of starch with different agitation speeds: agitation of T-CNF suspension + T-CNF/starch mixture agitation.

sample and the separation of the microfibrils from the bundles. M-CMFs, with a lower content of nanofibrils compared to M-CMNFs, exhibit the maximum AR at 5000 s^{-1}. The agitation favours the formation of microfibrils networks around the primary fibers, contributing to an increase in the AR. Though, at the same time, some fibrils are separated from the main backbones, which can be associated to a decrease of the AR. From 5000 s^{-1} onwards, although both effects continue to coexist, the AR slightly decreases, indicating a prioritization of the separation of microfibrils over their formation within the main structures. Besides, intense agitation of refined pulps may cause the fibers to curl, leading to a decrease of the AR [46]. As for the M-CMNFs, the combination of both mechanical treatments (refining and HPH) induced a more pronounced defibrillation effect, which persisted even at high agitations. As a result, a spongier and stretching network was formed between the nanofibrils, without even breaking the networks.

Fig. 3 shows the particle size distribution of M-CMFs, M-CMNFs and T-CNFs at different stirring speeds using the LDS technique, which primarily measures the microscale fraction (> 0.5 μm) and the aggregates produced. LDS is a technique more suitable for spherical particles, and the results obtained in volume percentage may underestimate the actual equivalent fibril length [47]. In fact, the technique provides an equivalent spherical diameter, assuming that the light scattering pattern of the material is identical to that of spherical particles [35]. Nevertheless, the technique is useful to compare the relative "size" of different samples, such as CMNFs at different agitation speeds. Fig. 3a, c and e present the volume distributions, providing an indication of the size of the bigger fibrils or aggregates that are present in smaller quantities, as can be seen in the number distributions (Fig. 3b, d and f), where the large aggregates observed in the volume distributions, which correspond to a relative low number of particles, disappear.

For M-CMFs, Fig. 3a and b show that at 300 s^{-1} the percentage of larger particles is slightly higher. Although small, this difference is relevant for the application of the CMFs in coatings. After 5000 s^{-1} of agitation, for which the maximum aspect ratio is obtained, the amount of these bigger "particles" decreases, most certainly due to their fibrillation. Further, an increase in speed up to 40,000 s^{-1} does not result in a

Table 5
Mechanical properties of base paper coated with 20 % of T-CNFs and 80 % of starch.

	Tensile Index (Machine Direction) (kN·m/kg)	Tensile Index (Cross Direction) (kN·m/kg)	Burst Index (kPa·m^2/g)	Tear Index (mN·m^2/g)	Gurley air resistance (s)
Base paper	35.3 ± 1.8^{a}	26.6 ± 1.6^{a}	1.56 ± 0.13^{a}	10.28 ± 0.39^{a}	1.5 ± 0.1^{a}
300 s^{-1} + 300 s^{-1}	41.3 ± 3.0^{b}	30.5 ± 2.0^{b}	2.32 ± 0.18^{b}	10.78 ± 0.35^{b,c}	697 ± 504^{c}
300 s^{-1} + 5000 s^{-1}	40.8 ± 2.1^{b}	33.5 ± 0.7^{d}	2.39 ± 0.14^{b}	10.79 ± 0.51^{b,c}	1097 ± 189^{c}
5000 s^{-1} + 300 s^{-1}	42.2 ± 3.4^{b}	30.4 ± 2.3^{b}	2.40 ± 0.14^{b}	10.86 ± 0.46^{c}	1044 ± 673^{c}
5000 s^{-1} + 800 s^{-1}	41.5 ± 0.6^{b}	31.0 ± 2.1^{b,c}	2.37 ± 0.15^{b}	10.39 ± 0.19^{a,b}	1057 ± 20^{c}
5000 s^{-1} + 5000 s^{-1}	42.5 ± 2.2^{b,c}	33.1 ± 2.1^{c,d}	2.51 ± 0.10^{c}	10.56 ± 0.47^{a,b}	1239 ± 407^{c}
40,000 s^{-1} + 5000 s^{-1}	**44.5 ± 0.5^{c,d}**	**33.7 ± 0.8^{d}**	**2.56 ± 0.10^{c}**	**11.00 ± 0.42^{c}**	**1075 ± 119^{c}**
Only Starch 300 s^{-1} (4 % solids)	45.4 ± 0.4^{d}	34.3 ± 0.5^{d}	2.75 ± 0.11^{d}	10.25 ± 0.43^{a}	21 ± 4^{b}
Only Starch 300 s^{-1} (6 % solids)	49.1 ± 2.2^{c}	39.4 ± 0.8^{b}	3.09 ± 0.14^{c}	10.59 ± 0.12^{a,b}	421 ± 70^{c}
Only Starch 5000 s^{-1} (6 % solids)	45.1 ± 0.9^{b}	38.0 ± 2.1^{b}	2.69 ± 0.11^{b}	10.44 ± 0.18^{a,b}	83 ± 4^{b}

Bold row means the best mechanical properties.

significant variation in size, as similar results are observed despite the reduction in the AR due to sedimentation. This indicates that it is possible to separate the microfibrils from the bundles without breaking the fibers. M-CMNFs show a similar distribution to M-CMFs at 300 s^{-1} but with a lower fraction of bigger particles (Fig. 3c). By increasing the agitation speed, a shifting of the fiber distribution towards smaller values is visible in Fig. 3d, indicating that not only homogenization, but also agitation, contribute to the dispersion effect by separating the fibrils to a greater extent than breaking them apart.

Finally, T-CNF that is in a gel state exhibits higher viscosity than the other CMNFs that are liquid suspensions. Therefore, when a portion of T-CNF gel is added to water, this is not easily dispersed in the liquid, presenting clusters and aggregates in the macroscale, which require a strong agitation to disperse the fibrils in water. These aggregates are visible in Fig. 3e and f at 300 s^{-1}, resulting in higher size values. Similarly to the M-CMNFs, an increase of the stirring speed shifts the fiber size distribution towards smaller sizes. This suggests that the aggregates in the sample are breaking up and dispersing more evenly throughout the sample. For higher stirring speeds, above 800 s^{-1}, there is a modification of the fiber size distribution, with a noticeable reduction in size towards a lower size range. This indicates the elimination of the largest clusters for speeds above 800 s^{-1}. For 40,000 s^{-1}, the peak appearing in the number distribution is reduced to 2 μm (Fig. 3f), representing a two orders of magnitude difference compared to the initial sample. In addition, the presence of a high number of nanofibrils in the TEM images, prepared with agitation to dilute and disperse the hydrogels, suggests that a portion of the sample is below the limit of detection of the LDS (under 500 nm). Therefore, to see this fraction, Fig. 4 shows the DLS distribution of the T-CNFs stirred at 40000 s^{-1} without and with pulsed sonication for 1 min. In the first case, two ranges of diameters are observed, with the larger range aligned with the peak in Fig. 3f at around 2 μm. When sonication was applied to fully disperse the aggregates, the larger particles disappear and a new peak between 25 and 75 nm becomes visible, representing the most nanofibrillated part of the suspension, and in accordance with the diameter of the fibrils in TEM [48].

Starch is the other compound used in the coatings, aiming at improving the mechanical properties of the base papers. The starch suspension was prepared by cooking until its complete dissolution, obtaining a viscous suspension. Starch suspensions have been extensively studied in the last decades, considering several parameters such as temperature, solid concentration or amylose concentration [49,50]. In the present work, the way agitation affects the rheology of starch and starch-CMNF suspensions was studied.

Fig. 5 shows the differences in the rheological behaviour of starch suspensions at different agitation speeds during the cooking process at 90 °C for 10 min. Starch suspension at 10 wt% are too viscous to be applied as a coating layer, making it unsuitable for coating base papers. On the contrary, suspensions at 4 wt% of starch are too liquid for the same purpose. For a given constant solids concentration and shear rate, the shear stress decreases by increasing the agitation speed from 300 s^{-1} up to 800 s^{-1}, which leads to a considerable decrease in viscosity. On the other hand, from 800 s^{-1} agitation speed onwards, the rheology of the

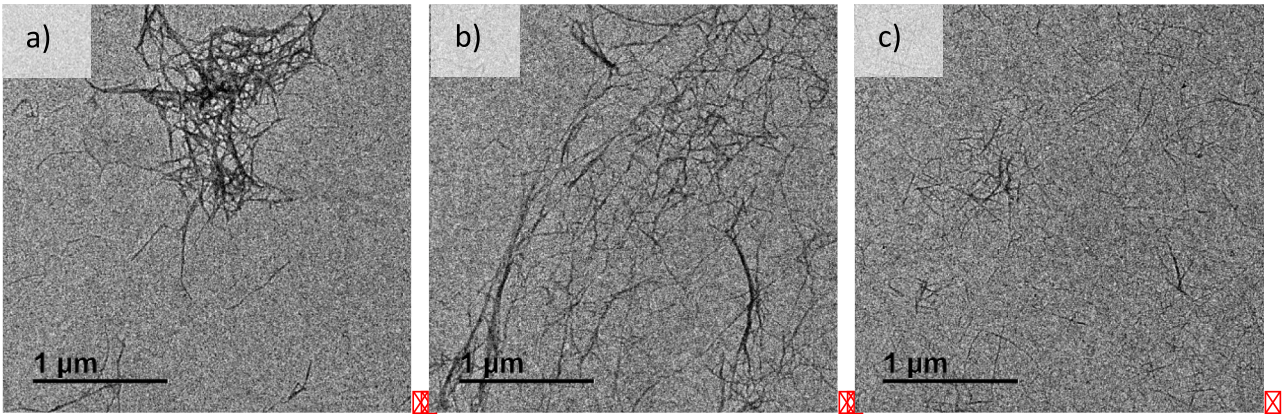

Fig. 11. TEM images of T-CNFs stirred at different agitations: a) 800 s^{-1}; b) 5000 s^{-1}; c) 40,000 s^{-1}.

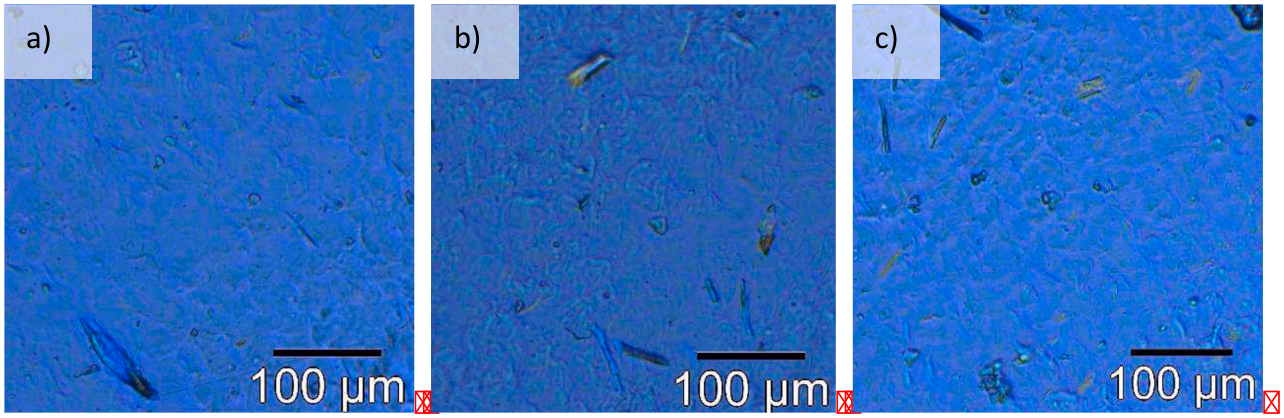

Fig. 12. Optical microscopy of coatings prepared at 4 wt% of total solids with 20 wt% of T-CNFs and 80 wt% of starch with different T-CNF and mixture agitation speeds: a) 300 s^{-1} + 300 s^{-1}; b) 800 s^{-1} + 800 s^{-1}; c) 5000 s^{-1} + 5000 s^{-1}.

samples shows minimal differences regardless the solids concentrations.

When comparing the mechanical properties of papers coated with starch formulations stirred at 300 and 5000 s^{-1} (Table 2), it is visible a higher tensile index for the low agitation. In addition, the samples with 6 wt% of solids have a better tensile index then those with 8 wt%. This suggests that starch coatings improve the tensile index, but this effect decrease with the amount of solids. In Table 2 it is also visible that both the stirring speed and the solids content also impact on the thickness of the coating layer and on the paper air resistance: higher solids content results in thicker coatings and reduce the porosity, whereas higher stirring speeds, which lead to less viscous starch formulations, have the opposite effect. Furthermore, the tear index remains consistent across all cases.

The rheology of the coating suspensions prepared with mixtures of M-CMFs and starch was studied, considering different agitation speeds of the M-CMFs and starch/M-CMFs (Fig. 6). A Bingham pseudoplastic behaviour is observed in coatings prepared with starch and M-CMFs as shown by Li et al. 2021 [51], whereas coatings containing only starch with the same total solids content (6 wt%) exhibit a pseudoplastic behaviour without yield stress. The viscosity is higher for M-CMFs coatings than for coatings with starch alone, indicating that the cellulose materials can be used to increase the viscosity of the coatings or to reduce the total solids in the coating.

The increase of the agitation speed of the mixture from 300 s^{-1} to 5000 s^{-1} leads to a decrease in the viscosity of the formulations with M-CMFs stirred under the same conditions as the starch alone formulations, as it was already observed for the latter. Furthermore, when the mixture agitation speed is maintained at 5000 s^{-1}, the increase of the initial agitation of M-CMFs results in a decrease in viscosity with the agitation speed, as depicted by the blue line in Fig. 6 (until 5000 s^{-1}). This corresponds to an agitation close to the maximum aspect ratio, as shown in Fig. 3. Nevertheless, higher agitation of the M-CMFs (40,000 s^{-1}, green line) results in the separation of the microfibrils from the main structures, forming independent networks. This separation increases the viscosity, despite the decrease in the aspect ratio.

Table 3 presents the mechanical properties of the papers coated with starch or starch/CMNFs. Equal superscripts for the same property indicate samples with no significant differences according to the Multiple Range Test. The use of starch/CMNF coatings, prepared under optimal agitation conditions, leads to a significant increase in the tensile index (in relation to the base paper), up to 59 % and 76 % in machine and in cross direction, respectively. However, the presence of M-CMFs in the coating formulations has varying effects on the mechanical properties, depending on the agitation speed, which emphasizes the importance of the CMNFs dispersion.

Using 300 s^{-1} for the mixture agitation, the presence of M-CMFs produces minimal increments in the tensile and burst indexes, compared to the starch coated paper (with starch stirred also at 300 s^{-1}). On the contrary, for papers coated with mixtures stirred at 5000 s^{-1}, the opposite occurs: the tensile index increases 24 % in the machine direction compared to the papers coated with starch alone using various fibrils agitation speeds. As for the cross direction, the best results in the tensile index were obtained with 5000 s^{-1} + 5000 s^{-1}, with an increase of 23 % in respect to starch coated base papers. This condition also yields the highest burst index, with an increase of 140 % and 39 % compared to the base paper and to the starch coated papers, respectively. Notably, high agitation conditions of M-CMF (40,000 s^{-1}) did not lead to an increase in the burst or tensile indexes in the cross direction, being the optimal agitation for M-CMFs the one corresponding to the minimum gel point.

Fig. 7 shows the images of these coatings, obtained by optical microscopy. At 5000 s^{-1} + 5000 s^{-1} agitation (Fig. 7b), CMFs form networks from primary backbones, with smaller fibrils emerging. However, at higher agitation of the fibrils (40,000 s^{-1} + 5000 s^{-1}), a separation of the fibrils occurs, leading to the breaking of the networks and a reduction of the tensile index in the cross direction (−15 %), burst index (−7 %) and tear index (−4 %). Only the tensile index in the machine direction is significantly the same according to the multiple range test. On the other hand, low agitation speeds (300 s^{-1} + 300 s^{-1}) result in a less uniform distribution of fibrils throughout the coating with some aggregates observed and the mechanical properties are far from the obtained in the optimal dispersion of M-CMFs. The mechanical properties of this coating are more closed to the obtained using only starch at the same agitation, which indicate the no effectivity of non-dispersed M-CMFs.

Considering the deviations, minimal differences of the tear index between the base paper, the samples coated only with starch, and those coated with the mixture of M-CMFs and starch are detected. According to the multiple range test, only the specific condition already mentioned (5000 s^{-1} + 5000 s^{-1}) is significantly different (the tear index is 6 % higher than the sample coated only with starch). As expected, the Gurley air resistance has its maximum for the sample with the best mechanical properties.

The aforementioned findings confirm that the best mechanical properties are achieved when the viscosity of the coatings decreases. Therefore, the optimal stirring conditions for the coating can be selected by identifying the lowest viscosity. This approach eliminates the need for paper handsheet preparation and subsequent analysis of their properties, providing a more efficient and practical method for optimizing the coating process.

The second type of CMNFs studied, the M-CMNFs, which were obtained by refining and high-pressure homogenization (HPH), form a 3D spongy network after passing through the HPH without the need of agitation. The rheology of coatings prepared with CMNFs and starch is

shown in Fig. 8. Similarly to the M-CMFs, when starch and M-CMNFs are combined, the coatings exhibit a Bingham pseudoplastic behaviour, while maintaining the constant total solids content (6 wt%). The viscosity of the coatings with M-CMNFs is similar to that of the coatings containing M-CMFs. However, there are notable differences of the viscosity for different agitation speeds. In fact, the agitations below 800 s^{-1} + 800 s^{-1} maintain the viscosity of the coating but an increase of the mixture agitation up to 5000 s^{-1} (800 s^{-1} + 5000 s^{-1}) leads to a decrease the viscosity. However, when M-CMNFs are stirred more strongly, the viscosity increases again (blue and green line in Fig. 8). So, in this case, it seems that a direct relationship between the AR or gel point of M-CMNFs and the rheology of the mixture cannot be found. However, it is observed that the best agitation speed identified for the M-CMFs mixture is also suitable for M-CMNFs, indicating that the second agitation stage may be the most important for the coating preparation.

As before, for the coatings containing CMNFs, low viscosity values correspond to the best mechanical properties of the papers (Table 4). In fact, the coatings with the lower viscosity values (800 s^{-1} + 5000 s^{-1}) exhibit the highest values of tensile index in both machine and cross direction, as well as burst index, with increments of 26, 19 and 47 %, respectively, compared to the paper coated only with starch at the same agitation. These results are better than those obtained with M-CNFs, indicating that the additional homogenization step has a positive impact on the final mechanical properties of papers. When comparing different agitation conditions, the increase in the mechanical properties varies between 48 and 71 % for the tensile index, and between 121 and 154 % for the burst index, compared to the base paper. Optical microscopy images of these coatings (Fig. 9) reveal that at low agitations (300 s^{-1} + 300 s^{-1}), CMNFs are already branched. As the agitation increases to 800 s^{-1} + 5000 s^{-1} (Fig. 9b), CMNFs become more separated but still maintain the primary backbones from which the networks are produced. This union of the primary backbones and the micro/nanofibrils causes networks to form that improve mechanical performance up to the best values in all mechanical properties studied. However, higher agitation of fibrils (40,000 s^{-1} + 5000 s^{-1}) in Fig. 9c leads to a separation of the microfibrils, disturbing the networks and resulting in a reduction of the mechanical resistances. Nevertheless, fibril shortening is not visible (as it is in Fig. 2), and so the aspect ratio remains almost constant for the highest agitations. On the other hand, the tear index does not differ significantly from that of the base papers coated only with starch, while the Gurley air resistance is much higher for the samples with a mixture agitation of 5000 s^{-1}, indicating a decrease in porosity.

The rheology of the coatings prepared with T-CNFs (20 %) and starch (80 %) is shown in Fig. 10, measured at different stirring speeds. Since a 6 wt% of total solids resulted in a high viscosity that hinders the application on the coating machine, the samples were prepared at 4 % of total solids. Despite this reduction of the solids content, the coatings with T-CNF also exhibit a Bingham pseudoplastic behaviour, with a yield stress ranging from 50 to 100 Pa, higher than those observed for M-CMF and M-CMNF coatings (yield stresses below 50 Pa). As a result, higher external forces were required in the coating machine to achieve a homogeneous coating layer, making it challenging to apply T-CNF coatings [52].

The viscosity values at 4 wt% of solids using T-CNFs and starch are in the same range as those of the mechanical CMNFs prepared using 6 wt% of solids. Both an increase in T-CNF agitation and in the agitation of the starch/T-CNF mixture led to a decrease of the viscosity. On the other hand, coatings produced only with starch at 4 wt% are too liquid like, making it difficult to coat the base paper, due to the absorption by the base paper. For this technical reason, it was only possible to measure the mechanical properties of the coating with 4 wt% of starch at 300 s^{-1}. Table 5 lists also the mechanical properties of coating with starch at 4 wt % of solids.

As for the mechanical properties, the use of T-CNFs did not result in any improvement in tensile and burst properties at any of the studied agitations, in contrast to the use of the mechanical CNMFs. This observation is in line with previous findings in the bulk application of CNFs, in which papers reinforced with the chemically pretreated CNFs did not exhibit as good mechanical properties as papers reinforced with CMNFs obtained solely by mechanical treatments [53–55]. The T-CNF networks are composed of short fibrils which form entanglements, as depicted in Fig. 11. However, the poor degree of fibrillation makes fibril networks more prone to disentanglement with agitation, with a maximum aspect-ratio value at low agitations, around 450 s^{-1} (as illustrated in Fig. 2).

In this case, the presence of T-CNFs had a pronounced negative influence on the mechanical properties compared with the papers coated only with starch, particularly at the agitation condition of 300 s^{-1} + 300 s^{-1}, for which the properties are most negatively affected, coinciding with the maximum AR. For these T-CNF coatings, the tear index is slightly higher than for the starch coatings and the air resistance has a relevant decrease, again influenced by the agitation speed, which promotes the separation of the T-CNF aggregates. Finally, optical microscopy images (Fig. 12) reveal the presence of a small fraction of T-CNFs that are not effectively nanofibrillated. These microfibrils seem more separated after 4000 s^{-1} of agitation.

4. Conclusions

The dispersion of CMNF suspensions prior to their application has been identified as a critical parameter for enhancing the paper properties by starch-based coating formulations. For a given composition, it is important to optimize the dispersion degree of the CMNFs before its use and the mixture agitation of CMNFs/starch to obtain a minimum viscosity of the coating formulation and thus a maximum paper reinforced effect. Therefore, rheological data of the coatings can be used to optimize the quality of coated papers by selecting the best dispersion degree without the need of actual application on the paper.

When comparing different types of CMNFs, it was found that coated paper prepared with mechanically pretreated CMNFs exhibit better mechanical properties while the coating had the lowest viscosity compared to the use of chemically oxidized CMNFs, at the same percentage of solids. The latter showed higher viscosity and required a lower percentage of solids for the coating formulation. It is concluded that a comprehensive understanding of CMNF dispersion is essential for effectively controlling products that incorporate CMNFs, as well as for understanding one of the factors contributing to scaling up the CMNF manufacturing process. This issue requires further research for the different applications.

CRediT authorship contribution statement

JL. Sanchez-Salvador: Investigation, Methodology, Formal analysis, Writing – Original Draft; MG. Rasteiro: Supervision, Resources and Writing – Review & Editing; A. Balea: Investigation and Formal analysis; M. Sharma: Methodology, Investigation and Writing – Review & Editing; JFS. Pedrosa: Methodology, Investigation and Software; C. Negro: Conceptualization, Funding acquisition and Writing – Review & Editing. MC. Monte: Supervision & Conceptualization; A. Blanco: Supervision, Conceptualization, Project administration and Writing – Review & Editing; PJT. Ferreira: Supervision, Formal analysis and Writing – Review & Editing.

Authors declare that in this work we have not involve any human subjects.

Authors declare no competing interests.

Authors declare we have read the information on Ethics in publishing.

Declaration of competing interest

The authors declare that they have no known competing financial interests or personal relationships that could have appeared to influence

the work reported in this paper.

Acknowledgments

The authors want to thank the financial support by the Science and Innovation Ministry of Spain (projects PID2020-113850RB-C21 "CONFUTURO-ES" and PDC2021-120964-C21 "VALORCON") as well as the grant from the Universidad Complutense de Madrid (EB27/21) for the stay of J.L Sanchez-Salvador at the University of Coimbra. In addition, the Strategic Research Centre Project UIDB00102/2020, funded by FCT, is acknowledged.

References

[1] G.P. Udayakumar, S. Muthusamy, B. Selvaganesh, N. Sivarajasekar, K. Rambabu, F. Banat, S. Sivamani, N. Sivakumar, A. Hosseini-Bandegharaei, P.L. Show, Biopolymers and composites: properties, characterization and their applications in food, medical and pharmaceutical industries, Journal of Environmental Chemical Engineering 9 (4) (2021), 105322.
[2] T.C. Mokhena, M.J. John, Cellulose nanomaterials: new generation materials for solving global issues, Cellulose 27 (2020) 1149–1194.
[3] C. Negro, A. Balea, J.L. Sanchez-Salvador, C. Campano, E. Fuente, M.C. Monte, A. Blanco, Nanocellulose and its potential use for sustainable industrial applications, Latin American Applied Research-An international journal 50 (2) (2020) 59–64.
[4] S.H. Osong, S. Norgren, P. Engstrand, Processing of wood-based microfibrillated cellulose and nanofibrillated cellulose, and applications relating to papermaking: a review, Cellulose 23 (1) (2016) 93–123.
[5] J. Pennells, I.D. Godwin, N. Amiralian, D.J. Martin, Trends in the production of cellulose nanofibers from non-wood sources, Cellulose 27 (2) (2020) 575–593.
[6] S.R. Djafari Petroudy, B. Chabot, E. Loranger, M. Naebe, J. Shojaeiarani, S. Gharehkhani, B. Ahvazi, J. Hu, S. Thomas, Recent advances in cellulose nanofibers preparation through energy-efficient approaches, A Review, Energies 14 (20) (2021) 6792.
[7] H. Kargarzadeh, M. Mariano, J. Huang, N. Lin, I. Ahmad, A. Dufresne, S. Thomas, Recent developments on nanocellulose reinforced polymer nanocomposites: a review, Polymer 132 (2017) 368–393.
[8] M. Jorfi, E.J. Foster, Recent advances in nanocellulose for biomedical applications, J. Appl. Polym. Sci. 132 (14) (2015) 14719.
[9] R. Bardet, J. Bras, Cellulose nanofibers and their use in paper industry, handbook of green materials: 1 bionanomaterials: separation processes, characterization and properties, World Scientific (2014) 207–232.
[10] A. Balea, M.C. Monte, N. Merayo, C. Campano, C. Negro, A. Blanco, Industrial application of nanocelluloses in papermaking: a review of challenges, technical solutions, and market perspectives, Molecules 25 (3) (2020) 526.
[11] J.L. Sanchez-Salvador, A. Balea, C. Negro, M.C. Monte, A. Blanco, Gel point as measurement of dispersion degree of Nano-cellulose suspensions and its application in papermaking, Nanomaterials-Basel 12 (5) (2022) 790.
[12] S. Omori, T. Morita, K. Matsumoto, A. Nagatani, T. Tanaka, Influence of Agitation Equipment on Reinforcing Effect and Dispersion State of Cellulose Nano-Fibers in Natural Rubber, Trans Tech Publ, Key Engineering Materials, 2017, pp. 23–26.
[13] Y. Tan, Y. Liu, W. Chen, Y. Liu, Q. Wang, J. Li, H. Yu, Homogeneous dispersion of cellulose nanofibers in waterborne acrylic coatings with improved properties and unreduced transparency, ACS Sustain. Chem. Eng. 4 (7) (2016) 3766–3772.
[14] C. Campano, N. Merayo, A. Balea, Q. Tarres, M. Delgado-Aguilar, P. Mutje, C. Negro, A. Blanco, Mechanical and chemical dispersion of nanocelluloses to improve their reinforcing effect on recycled paper, Cellulose 25 (1) (2018) 269–280.
[15] S. Parveen, S. Rana, R. Fangueiro, A review on nanomaterial dispersion, microstructure, and mechanical properties of carbon nanotube and nanofiber reinforced cementitious composites, J. Nanomater. 2013 (2013), 710175.
[16] T. Saito, S. Kimura, Y. Nishiyama, A. Isogai, Cellulose nanofibers prepared by TEMPO-mediated oxidation of native cellulose, Biomacromolecules 8 (8) (2007) 2485–2491.
[17] A. Isogai, Development of completely dispersed cellulose nanofibers, Proceedings of the Japan Academy, Series B 94 (4) (2018) 161–179.
[18] S.M. Fadel, W.S. Abou-Elseoud, E.A. Hassan, S. Ibrahim, M.L. Hassan, Use of sugar beet cellulose nanofibers for paper coating, Ind. Crop. Prod. 180 (2022), 114787.
[19] S.M. Mazhari Mousavi, E. Afra, M. Tajvidi, D. Bousfield, M. Dehghani-Firouzabadi, Cellulose nanofiber/carboxymethyl cellulose blends as an efficient coating to improve the structure and barrier properties of paperboard, Cellulose 24 (2017) 3001–3014.
[20] M. Sharma, R. Aguado, D. Murtinho, A.J. Valente, P.J. Ferreira, Micro-/nanofibrillated cellulose-based coating formulations: a solution for improving paper printing quality, Nanomaterials-Basel 12 (16) (2022) 2853.
[21] H. Xu, J.L. Sanchez-Salvador, A. Balea, A. Blanco, C. Negro, Optimization of reagent consumption in TEMPO-mediated oxidation of Eucalyptus cellulose to obtain cellulose nanofibers, Cellulose 29 (12) (2022) 6611–6627.
[22] ISO, ISO 5263-1:2004 Pulps — Laboratory wet disintegration — Part 1: Disintegration of chemical pulps, (2004).
[23] ISO, ISO 5264-2:2011 Pulps — Laboratory beating — Part 2: PFI mill method, (2011).
[24] M.E. Vallejos, F.E. Felissia, M.C. Area, N.V. Ehman, Q. Tarrés, P. Mutjé, Nanofibrillated cellulose (CNF) from eucalyptus sawdust as a dry strength agent of unrefined eucalyptus handsheets, Carbohyd Polym 139 (2016) 99–105.
[25] ISO, ISO 5351:2010 Pulps — Determination of limiting viscosity number in cupri-ethylenediamine (CED) solution, 2010.
[26] Y. Habibi, H. Chanzy, M.R. Vignon, TEMPO-mediated surface oxidation of cellulose whiskers, Cellulose 13 (6) (2006) 679–687.
[27] F. Serra-Parareda, R. Aguado, Q. Tarrés, P. Mutjé, M. Delgado-Aguilar, Potentiometric back titration as a robust and simple method for specific surface area estimation of lignocellulosic fibers, Cellulose 28 (2021) 10815–10825.
[28] TAPPI, TAPPI T 211 om-16:2016 Ash in Wood, Pulp, Paper and Paperboard: Combustion at 525 Degrees C, Peachtree Corners, GA, 2016.
[29] C. Campano, A. Balea, Á. Blanco, C. Negro, A reproducible method to characterize the bulk morphology of cellulose nanocrystals and nanofibers by transmission electron microscopy, Cellulose 27 (9) (2020) 4871–4887.
[30] D. Martinez, K. Buckley, S. Jivan, A. Lindstrom, R. Thiruvengadaswamy, J. Olson, T. Ruth, R. Kerekes, Characterizing the Mobility of Papermaking Fibres during Sedimentation, the Science of Papermaking: Transactions of the 12th Fundamental Research Symposium, Oxford. The Pulp and Paper Fundamental Research Society, Bury, UK, 2001, pp. 225–254.
[31] J.L. Sanchez-Salvador, M.C. Monte, C. Negro, W. Batchelor, G. Garnier, A. Blanco, Simplification of gel point characterization of cellulose nano and microfiber suspensions, Cellulose 28 (2021) 6995–7006.
[32] A. Celzard, V. Fierro, R. Kerekes, Flocculation of cellulose fibres: new comparison of crowding factor with percolation and effective-medium theories, Cellulose 16 (6) (2009) 983–987.
[33] R. Kerekes, C. Schell, Regimes by a crowding factor, J. Pulp Pap. Sci 18 (1992) J32–J38.
[34] J.F. Pedrosa, M.G. Rasteiro, C.P. Neto, P.J. Ferreira, Effect of cationization pretreatment on the properties of cationic Eucalyptus micro/nanofibrillated cellulose, Int. J. Biol. Macromol. 201 (2022) 468–479.
[35] J.A. Gamelas, J. Pedrosa, A.F. Lourenço, P. Mutjé, I. González, G. Chinga-Carrasco, G. Singh, P.J. Ferreira, On the morphology of cellulose nanofibrils obtained by TEMPO-mediated oxidation and mechanical treatment, Micron 72 (2015) 28–33.
[36] F. Storti, F. Balsamo, Particle size distributions by laser diffraction: sensitivity of granular matter strength to analytical operating procedures, Solid Earth 1 (1) (2010) 25–48.
[37] ISO, ISO 5636-3:2013 Paper and board — Determination of air permeance (medium range) — Part 3: Bendtsen method, (2013).
[38] ISO, ISO 1924-3:2005 Paper and board — Determination of tensile properties — Part 3: Constant rate of elongation method (100 mm/min), (2005).
[39] ISO, ISO 1974:2012 Paper — Determination of tearing resistance — Elmendorf method, (2012).
[40] ISO, ISO 2759:2014 Board — Determination of bursting strength, (2014).
[41] Z. Zai, M. Yan, C. Shi, L. Zhang, H. Lu, Z. Xiong, J. Ma, Cellulose nanofibrils (CNFs) in uniform diameter: capturing the impact of carboxyl group on dispersion and re-dispersion of CNFs suspensions, Int. J. Biol. Macromol. 207 (2022) 23–30.
[42] L. Kuutti, H. Pajari, S. Rovio, J. Kokkonen, M. Nuopponen, Chemical recovery in TEMPO oxidation, Bioresources 11 (3) (2016) 6050–6061.
[43] J.L. Sanchez-Salvador, C. Campano, A. Balea, Q. Tarrés, M. Delgado-Aguilar, P. Mutjé, A. Blanco, C. Negro, Critical comparison of the properties of cellulose nanofibers produced from softwood and hardwood through enzymatic, chemical and mechanical processes, Int. J. Biol. Macromol. 205 (2022) 220–230.
[44] R. Shinoda, T. Saito, Y. Okita, A. Isogai, Relationship between length and degree of polymerization of TEMPO-oxidized cellulose nanofibrils, Biomacromolecules 13 (3) (2012) 842–849.
[45] H.-N. Xu, Y.-H. Li, Decoupling arrest origins in hydrogels of cellulose nanofibrils, ACS omega 3 (2) (2018) 1564–1571.
[46] U.-B. Mohlin, Quality loss of refined softwood bleached Kraft pulp during agitated storage, Nord Pulp Pap Res J 25 (1) (2010) 76–81.
[47] A. Califice, F. Michel, G. Dislaire, E. Pirard, Influence of particle shape on size distribution measurements by 3D and 2D image analyses and laser diffraction, Powder Technol. 237 (2013) 67–75.
[48] A. Mandal, D. Chakrabarty, Isolation of nanocellulose from waste sugarcane bagasse (SCB) and its characterization, Carbohyd Polym 86 (3) (2011) 1291–1299.
[49] J.L. Doublier, Rheological studies on starch—flow behaviour of wheat starch pastes, Starch-Stärke 33 (12) (1981) 415–420.
[50] O.V. López, N.E. Zaritzky, M.A. García, Physicochemical characterization of chemically modified corn starches related to rheological behavior, retrogradation and film forming capacity, J. Food Eng. 100 (1) (2010) 160–168.
[51] M.C. Li, Q. Wu, R.J. Moon, M.A. Hubbe, M.J. Bortner, Rheological aspects of cellulose nanomaterials: governing factors and emerging applications, Adv. Mater. 33 (21) (2021) 2006052.
[52] T.G. Mezger, The Rheology Handbook: For Users of Rotational and Oscillatory Rheometers, Vincentz Network, 2006.
[53] J.L. Sanchez-Salvador, A. Balea, M.C. Monte, C. Negro, M. Miller, J. Olson, A. Blanco, Comparison of mechanical and chemical nanocellulose as additives to reinforce recycled cardboard, Sci. Rep. 10 (1) (2020) 1–14.
[54] L. Jiménez-López, M.E. Eugenio, D. Ibarra, M. Darder, J.A. Martín, R. Martín-Sampedro, Cellulose nanofibers from a dutch elm disease-resistant ulmus minor clone, Polymers 12 (11) (2020) 2450.
[55] A. Balea, N. Merayo, E. De La Fuente, C. Negro, A. Blanco, Assessing the influence of refining, bleaching and TEMPO-mediated oxidation on the production of more sustainable cellulose nanofibers and their application as paper additives, Ind. Crop. Prod. 97 (2017) 374–387.